

# Autofocusing MALDI mass spectrometry imaging of tissue sections and 3D chemical topography of nonflat surfaces

Mario Kompauer, Sven Heiles & Bernhard Spengler<sup>1</sup>

**We describe an atmospheric pressure matrix-assisted laser desorption–ionization mass spectrometry imaging system that uses long-distance laser triangulation on a micrometer scale to simultaneously obtain topographic and molecular information from 3D surfaces. We studied the topographic distribution of compounds on irregular 3D surfaces of plants and parasites, and we imaged nonplanar tissue sections with high lateral resolution, thereby eliminating height-related signal artifacts.**

In the fields of chemistry<sup>1</sup>, biology<sup>2</sup> and medicine<sup>3</sup>, interest in mass spectrometry imaging (MSI) performed under atmospheric pressure (AP) conditions in the sample region has grown rapidly. AP ionization techniques such as desorption electrospray ionization (DESI)<sup>4</sup> and matrix-assisted laser desorption–ionization (MALDI)<sup>5</sup> are sensitive tools for analyzing the chemical composition of surfaces. MALDI MSI<sup>6,7</sup> and DESI MSI<sup>8</sup> allow researchers to visualize the distribution of a plethora of compound classes from flat sample surfaces<sup>9</sup>. All current MSI techniques, however, have one major disadvantage in common: samples must be planar, roughly in the range of the lateral resolution; i.e., the aspect ratio must be about 1. Thus, rough surfaces or 3D objects can only be analyzed by using low lateral resolution and by sacrificing depth information or (in the case of MALDI or LDI) by using high laser energies for desorption. For example, rough surfaces of intact *Drosophila melanogaster*<sup>10</sup> and antibiotic substances from flattened *Streptomyces spp*<sup>11</sup> have been analyzed with lateral resolutions lower than 100  $\mu\text{m}$  without obtaining topographic information. Transmission-mode MALDI MSI experiments allow for lateral resolutions of about 1  $\mu\text{m}$ , as long as the sample height does not vary by more than  $\sim 1 \mu\text{m}$ <sup>12</sup>.

No available method allows researchers to simultaneously obtain topographic and chemical information with resolutions on the micrometer scale. Consequently, height, slope, angular

distribution, surface roughness, etc., can only be determined via topographical reconstruction from optical images before MSI experiments. The most prominent optical methods for topographic analysis of nonplanar surfaces, such as confocal scanning optical microscopy, are focus-detection based, as these methods enable noncontact measurements of samples<sup>13–15</sup>. The resulting optical images have spatial resolutions in the low-nanometer range, but no direct information about chemical surface composition is available from these measurements.

Here we report an autofocusing AP MALDI MSI system for studying 3D sample surfaces with topographic aspect ratios of up to 50. This system keeps the MALDI laser focus, fluence and ablation spot size constant over sample height variations by adjusting the sample stage position according to the sample height profile for each measurement spot, thus providing lateral resolutions of  $\leq 10 \mu\text{m}$  for 3D samples.

We implemented the autofocusing operation mode for MALDI experiments by introducing a laser triangulation system into the AP-SMALDI10 MSI system (**Fig. 1a**) on an orbital trapping mass spectrometer. The triangulation laser beam (**Fig. 1a**, 1) is focused to the same sample spot (2) as the MALDI laser beam (3), with an angle of  $35^\circ$  with respect to the mass spectrometer inlet axis (4). Light from the triangulation laser spot (5) is reflected over a mirror (6) and detected by a CMOS camera (7). The focal plane is determined based on the lateral position of the triangulation laser beam spot within the field of view, which allows the system to resolve 1.5- $\mu\text{m}$  height variations. The triangulation system has been integrated in the AP-SMALDI10 MSI source, which consists of the *xyz* sample positioning stage (8), the MALDI laser focusing optics (9) and the mass spectrometer inlet capillary (4). Autofocusing MSI increases the overall measurement time by about 25% compared to nonautofocusing MSI measurements. The working principle, experimental details and performance characteristics of the autofocusing AP MALDI MSI system are described in the Online Methods and in **Supplementary Note 1**.

The autofocusing MSI workflow is as follows. First, the sample was fixated on a MALDI target, and an optical microscopy image was acquired (**Fig. 1b**). Second, MALDI matrix was applied using a pneumatic sprayer (**Fig. 1c**). Third, AP MALDI MSI measurements were performed in autofocus mode, and this was followed by data processing, evaluation and visualization (**Fig. 1d–h**). Matrix application quality for 3D samples and ablation spot characterization in autofocusing mode are presented in **Supplementary Note 1**.

We illustrate the performance and workflow of the autofocusing MSI setup for a daisy petal (*Bellis perennis*) (**Fig. 1**). Three selected *m/z* images (average mass spectrum in **Fig. 1f**) are shown in **Figure 1g**, where they are color coded in red, green and blue. The

Institute of Inorganic and Analytical Chemistry, Justus Liebig University Giessen, Germany. Correspondence should be addressed to B.S. (bernhard.spengler@anorg.chemie.uni-giessen.de).

RECEIVED 9 FEBRUARY; ACCEPTED 31 JULY; PUBLISHED ONLINE 18 SEPTEMBER 2017; DOI:10.1038/NMETH.4433

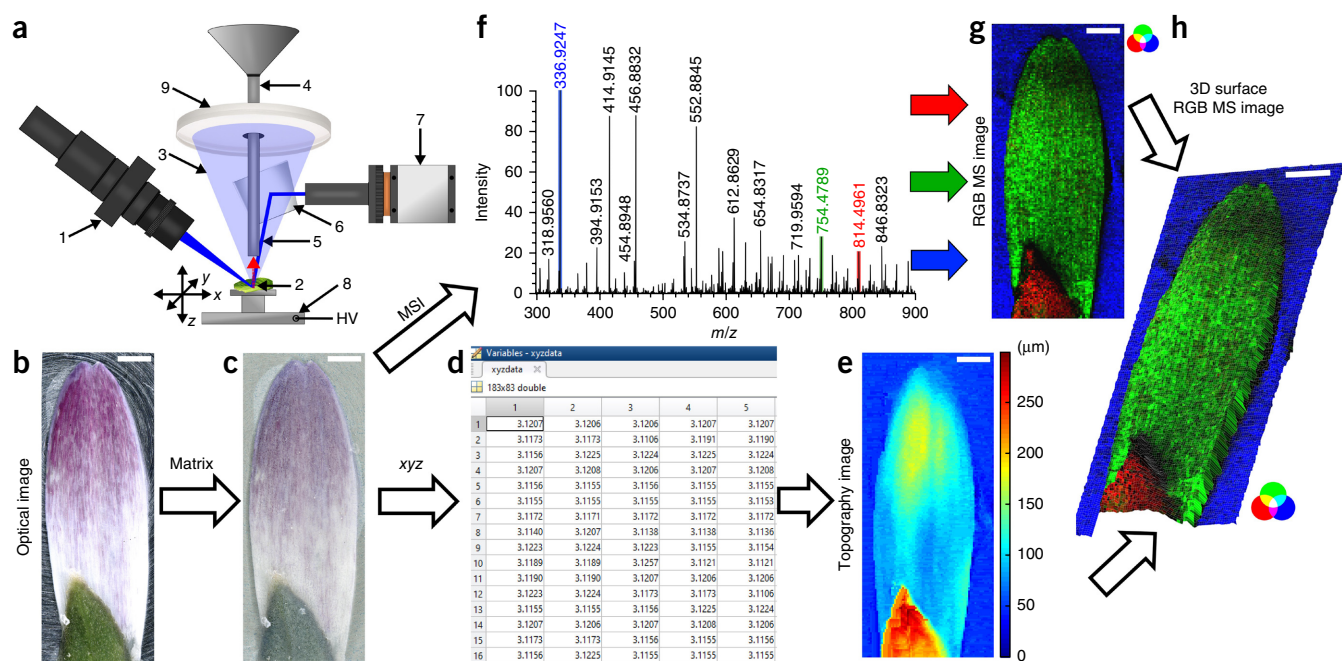


**Figure 1** | The autofocusing AP MALDI MSI system and workflow. (a) Scheme of the MSI setup (described in the text). Objects are not to scale. (b) Optical microscope image of a daisy petal (*Bellis perennis*). (c) Optical microscope image of the daisy petal after matrix application. (d) Topographical data stored in an xyz data matrix. (e) Topography image. (f) Average mass spectrum of the sample shown in c. The  $m/z$  values used for the RGB MS image (g) are color coded (g) RGB MS image of [saponin +  $\text{NH}_4$ ] $^+$  at  $m/z$  814.4961 (red), [PE(34:2) + K] $^+$  at  $m/z$  754.4789 (green) and  $m/z$  336.9247 (blue). (h) 3D surface RGB MS image. All scale bars are 1 mm.

data set contained a total of 1,277 assignable ion signals. **Figure 1g** shows that [saponin +  $\text{NH}_4$ ] $^+$  (red) was located exclusively in the green part of the sample. This compound is known to be present in the flowers of *B. perennis*<sup>16</sup>. Phosphatidylethanolamine [PE(34:2) + K] $^+$  (green) was located in the white–red part of the daisy petal (**Fig. 1b**). This compound is known to be an abundant component of the lipid bilayer. A background signal from the MALDI metal target is shown in blue. The topography image (**Fig. 1e**), containing the height information, and the MS images (**Fig. 1g**) were combined into a 3D surface RGB MS image (**Fig. 1h**) as a multidimensional data representation via home-built MATLAB scripts (see Online Methods). Gray-scale images of **Figure 1** are provided in **Supplementary Figure 1**.

A METLIN database search of the 1,277 detected ion signals yielded 4,852 annotations (i.e., database search hits of endogenous compounds with mass errors <2 p.p.m.; **Supplementary Data**). The untargeted database search assigned peptides, lipids and metabolites, some of which are visualized in **Supplementary Figure 2** (see also **Supplementary Table 1**).

AP conditions allow the measurement of biological samples in a near-physiological state. We therefore applied the autofocusing AP MALDI MSI system to biological samples directly taken from the environment. **Figure 2** shows the optical microscope image of a clover leaf (*Trifolium repens*) (**Fig. 2a**), the corresponding topography image (**Fig. 2b**) and the 3D surface RGB MS image (**Fig. 2c**). Kaempferol-3-O-galactoside [trifolin + Na] $^+$  (red), a galactose-conjugated flavonol exhibiting antifungal and anticancer effects<sup>17</sup>, was found in high abundance in the veins of the clover leaf. The lipid [MGDG(36:6) + K] $^+$ , one of the most abundant polar lipids in the chloroplast thylakoids of oxygen-evolving photosynthetic organisms that does not form bilayers,

is visualized in the green color channel<sup>18</sup>. A background signal from the MALDI metal target is shown in blue.

**Figure 2d** shows the optical microscope image of a male trematode (*Schistosoma mansoni*) that causes the tropical disease schistosomiasis, which infected 207 million people in 2012 (ref. 19). Our autofocusing MSI approach allows researchers to study the chemical surface composition (average mass spectrum in **Supplementary Fig. 3**) of this parasite, and it may benefit future studies aiming to intervene in the parasite's reproductive cycle or to develop vaccines. **Figure 2e** shows the chemical surface distribution of [PC(36:1) + Na] $^+$  (red) located at the oral sucker and the testes; [PC(34:1) + Na] $^+$  (green) is distributed over the entire body with varying intensity, and a background signal is shown in blue. Tandem MS ( $\text{MS}^2$ ) experiments increase chemical specificity and so enable more accurate and reliable annotation of compounds than standard MS experiments.  $\text{MS}^2$  spectra of lipids from the surface of *Schistosoma mansoni* employing autofocusing MSI are shown in **Supplementary Figure 4**. Because of the ~250- $\mu\text{m}$  height variation of the sample (**Fig. 2f**), measurements without autofocusing would not have been possible.

Autofocusing can also benefit the high-throughput analysis of tissue sections by MSI. We imperfectly mounted a coronal mouse brain section, which we intentionally positioned at a small tilt with respect to the MS inlet axis (**Supplementary Fig. 5**). This model of a rapid sample mounting or of a rough sample surface resulted in a maximum height difference of ~100  $\mu\text{m}$  (tilt angle 1.1°) across the sample. We measured the mouse brain section with autofocusing either on (**Fig. 2g**, bottom) or off (**Fig. 2g**, top) (**Supplementary Fig. 6**). While we observed an intensity drop in the direction of the white arrow (**Fig. 2g**, bottom) for the nonautofocusing mode, autofocusing mode led to a constant ion

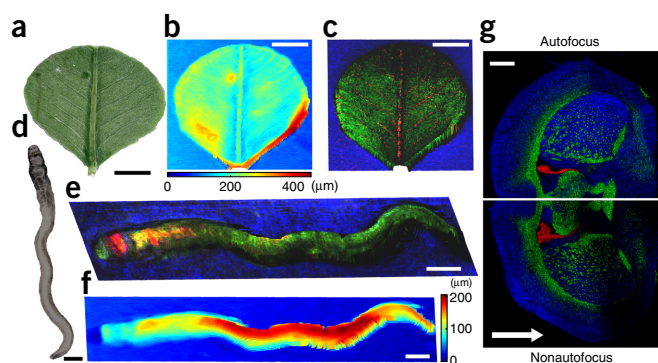


**Figure 2** | Autofocusing 3D surface profiling of plants, trematodes and mouse brain sections. (a) Optical microscope image of a clover leaf (*Trifolium repens*) before matrix application. (b) Topography image of the clover leaf. (c) 3D surface RGB MS image of [trifolin + Na]<sup>+</sup> at *m/z* 471.0905 (red), [MGDG(36:6) + K]<sup>+</sup> at *m/z* 813.4918 (green) and *m/z* 594.8937 (blue). (d) Optical microscope image of a trematode (*Schistosoma mansoni*) before matrix application. (e) 3D surface RGB MS image of [PC(36:1) + Na]<sup>+</sup> at *m/z* 810.5982 (red), [PC(34:1) + Na]<sup>+</sup> at *m/z* 782.5666 (green) and background at *m/z* 585.0636 (blue). (f) Topography image of the trematode. (g) RGB MS image of [SM(d40:2) + K]<sup>+</sup> at *m/z* 823.6084 (red), [PI-Cer(d38:0) + H]<sup>+</sup> at *m/z* 838.6159 (green) and [PC(40:7) + K]<sup>+</sup> at *m/z* 870.5410 (blue) from a coronal mouse brain section, with (upper half) and without (lower half) autofocusing. The scale bars are 2 mm (a–c), 200 μm (d–f) and 1 mm (g).

signal across the entire scanned area (Fig. 2g, top) on account of a constant ablation spot size and thus laser fluence for each single pixel. The red color channel represents [SM(d40:2) + K]<sup>+</sup>, localized in the lateral ventricle. [PI-Cer(d38:0) + H]<sup>+</sup> (green) is highly abundant in the corpus callosum, and [PC(40:7) + K]<sup>+</sup> (blue) represents the cerebral cortex. RGB MS images were visualized without needing total ion current (TIC) normalization, which is often used to counteract defocusing problems with the cost of biasing the analysis due to altered quantitative information for each pixel<sup>20</sup>. The effects of topography on MALDI MSI results are detailed in **Supplementary Note 2**. Gray-scale images of **Figure 2** are provided in **Supplementary Figure 7**.

In summary, we report a method to simultaneously obtain chemical and topographical surface images using autofocusing AP MALDI MSI. The field of potential applications ranges from chemistry, biology, medicine and the life sciences to quality inspections for targeted or untargeted chemical analysis of irregular 3D samples. Standard tissue-section MSI analysis can also be significantly improved through our method's ability to automate the focusing process and so provide undistorted chemical mapping at high lateral resolution across large tissue sections. The autofocusing approach can likely be implemented in various MSI setups.

## METHODS

Methods, including statements of data availability and any associated accession codes and references, are available in the [online version of the paper](#).

*Note: Any Supplementary Information and Source Data files are available in the online version of the paper.*

## ACKNOWLEDGMENTS

Financial support by the Deutsche Forschungsgemeinschaft (DFG) under grant SP314/13-1 and by the State of Hesse through LOEWE Center "DRUID" is gratefully acknowledged. S.H. thanks the Fonds der chemischen Industrie for a Liebig fellowship. The authors are grateful to W. Kummer (Institute of Anatomy and Cell Biology, Justus Liebig University Giessen, Germany) and his group members for providing mouse brain samples and to C. Grevelding (Institute for Parasitology, Justus Liebig University Giessen, Germany) for providing *Schistosoma mansoni* samples.

## AUTHOR CONTRIBUTIONS

B.S. designed and supervised the project; M.K. set up the new instrumentation, performed all experiments, and performed the data analysis; M.K., S.H. and B.S. discussed the findings and wrote the manuscript.

## COMPETING FINANCIAL INTERESTS

The authors declare competing financial interests: details are available in the [online version of the paper](#).

**Reprints and permissions information is available online at <http://www.nature.com/reprints/index.html>. Publisher's note: Springer Nature remains neutral with regard to jurisdictional claims in published maps and institutional affiliations.**

1. Yoshimura, Y., Goto-Inoue, N., Moriyama, T. & Zaima, N. *Food Chem.* **210**, 200–211 (2016).
2. Boughton, B.A., Thinagaran, D., Sarabia, D., Bacic, A. & Roessner, U. *Phytochem. Rev.* **15**, 445–488 (2016).
3. Longuespée, R. *et al. Prot. Clin. Appl.* **10**, 701–719 (2016).
4. Takáts, Z., Wiseman, J.M., Gologan, B. & Cooks, R.G. *Science* **306**, 471–473 (2004).
5. Laiko, V.V., Baldwin, M.A. & Burlingame, A.L. *Anal. Chem.* **72**, 652–657 (2000).
6. Spengler, B., Hubert, M. & Kaufmann, R. In *Proceedings of the 42nd Annual Conference on Mass Spectrometry and Allied Topics*, 1041 (1994).
7. Caprioli, R.M., Farmer, T.B. & Gile, J. *Anal. Chem.* **69**, 4751–4760 (1997).
8. Wiseman, J.M., Ifa, D.R., Song, Q. & Cooks, R.G. *Angew. Chem. Int. Ed.* **45**, 7188–7192 (2006).
9. Spengler, B. *Anal. Chem.* **87**, 64–82 (2015).
10. Kaftan, F. *et al. J. Mass Spectrom.* **49**, 223–232 (2014).
11. Kroiss, J. *et al. Nat. Chem. Biol.* **6**, 261–263 (2010).
12. Zavalin, A. *et al. J. Mass Spectrom.* **47**, 1473–1481 (2012).
13. Macdonald, D.A. *J. Archaeol. Sci.* **48**, 26–33 (2014).
14. Kim, K.W., Lee, S.-T., Bae, S.-W. & Kim, P.-G. *Microsc. Res. Tech.* **74**, 1166–1173 (2011).
15. Garzón, J., Gharbi, T. & Meneses, J. *J. Opt. A, Pure Appl. Opt.* **10**, 104028 (2008).
16. Wray, V., Kunath, A., Schöpke, T. & Hiller, K. *Phytochemistry* **31**, 2555–2557 (1992).
17. Kim, M.-J. *et al. Phytomedicine* **23**, 998–1004 (2016).
18. Gounaris, K. & Barber, J. *Trends Biochem. Sci.* **8**, 378–381 (1983).
19. Fenwick, A. *Public Health* **126**, 233–236 (2012).
20. Råföls, P. *et al. Mass Spec. Rev.* **2016**, 1–26 (2016).

## ONLINE METHODS

**Autofocusing high-resolution AP MALDI MSI system.** To perform surface profiling with the autofocusing AP MALDI MSI system, an AP-SMALDI10 MSI system (TransMIT GmbH, Giessen, Germany) was modified with an autofocusing unit. The experimental details and working principles of the AP-SMALDI10 MSI system are described elsewhere<sup>21,22</sup>. The autofocusing AP MALDI MSI system was coupled to an orbital trapping mass spectrometer (Q Exactive, Thermo Fisher Scientific GmbH, Bremen, Germany).

The developed autofocusing system consists of a triangulation laser (Flexpoint Laser Diode Module, 405 nm, 10 mW continuous wave, Laser Components GmbH, Olching, Germany), which irradiates the sample at an angle of 35° relative to the mass spectrometer transfer capillary axis. The sample was mounted on the *xyz* stage of an AP-SMALDI10 ion source (TransMIT GmbH, Giessen, Germany); this stage had a positioning precision of <10 nm. Focusing of the triangulation laser was performed with an optical system composed of an  $f = 75$  mm focusing lens, a neutral density filter (OD = 1) and an iris diaphragm. The triangulation laser beam profile at the focal point was characterized by a beam profiler system (Spiricon Inc., Logan, Utah, USA and CoHu Inc., San Diego, California, USA). The beam profiler setup is described in ref. 23. The triangulation laser spot was visualized with a CMOS USB camera (EO-1312C 1,280 × 1,024 pixels, Edmund Optics GmbH, Karlsruhe, Germany) equipped with a 4× magnification objective lens. The MALDI UV laser was focused with the centrally bored objective lens of the AP-SMALDI10 MSI system<sup>21,22</sup>. The generated ions were accelerated by an electric field toward the transfer capillary of the mass spectrometer. All functionalities of the AP-SMALDI10 MSI system and the autofocusing system were controlled by an in-house-developed MATLAB control program (**Supplementary Software**) (R2016a, The MathWorks GmbH, Ismaning, Germany).

**Working principle of the 3D surface profiling triangulation setup.** Triangulation laser and MALDI laser were focused onto the same spot on the sample, the MALDI laser coaxially (0°) and the triangulation laser with an angle of 35° with respect to the mass spectrometer inlet capillary axis. Focusing of the triangulation laser was performed with a neutral density filter, an iris aperture and an achromatic lens assembly. The spot of the triangulation laser light was imaged with a CMOS camera chip by means of a mirror and a 4× magnification objective lens. This triangulation setup allowed us to determine sample height differences relative to a predefined reference height. The reference sample height was defined by a position of the triangulation laser spot in the CMOS camera image as reference point. During scanning, the actual position of the laser spot was continuously determined by computing the centroid position of the imaged laser light spot. For MALDI MSI applications we chose this reference point to coincide with the focused MALDI laser position. Moving the sample stage out of the focal plane results in a shift  $\Delta$  of the triangulation laser spot. This relative shift  $\Delta$  between the triangulation laser spot centroid and the reference point allowed us to determine a conversion factor  $cf$  from the calibrated CMOS image magnification values. For our particular setup geometry, the height-shift conversion factor was determined as  $cf = 1.5 \mu\text{m}/\text{pixel}$ . After determining  $cf$ , this conversion factor was used to determine height differences

for samples with unknown topography by measuring the triangulation laser spot movement in the CMOS camera image. The depth resolution was limited to  $\Delta = 1$  pixel and consequently to  $1.5 \mu\text{m}$ . A theoretical maximum pixel-to-pixel height difference of  $\sim 960 \mu\text{m}$  results from the detector size of 1,280 pixels. In our experiments, pixel-to-pixel height differences of up to  $\sim 500 \mu\text{m}$  were successfully measured.

In autofocusing mode, the measured height differences were used to adjust the sample stage's *z*-position in an iterative procedure until the position of the triangulation laser spot centroid again coincided with the selected reference position within  $\pm 5 \mu\text{m}$ . By saving the resulting *z*-positions of the positioning stage for all pixels of the selected surface measurement raster, the topographic information of the sample surface was obtained. For MALDI MSI applications, autofocusing before every pixel measurement enables us to keep the laser ablation spot size (and thus laser fluence) constant across sample height differences and thus to perform MALDI MSI experiments of irregular 3D surfaces.

**Mass spectrometry imaging.** For a step-by-step protocol, please refer to the corresponding protocol file available as a **Supplementary Protocol** and at *Protocol Exchange*<sup>24</sup>.

**Sample preparation.** All plant samples were taken from the environment and glued, without any (pre-)preparation, onto a target using superglue (UHU Sekundenkleber, UHU GmbH, Bühl, Germany). Fresh frozen mouse samples (C57Bl6/N male and female mice aged 12 to 20 weeks) were cut into sections of 20  $\mu\text{m}$  thickness with a cryostat (HM525, Thermo Scientific, Dreieich, Germany) at  $-20^\circ\text{C}$ , thaw mounted onto standard targets and stored at  $-80^\circ\text{C}$  until MSI analysis. Mouse samples were provided by W. Kummer, Justus Liebig University Giessen. Adult *Schistosoma mansoni* were measured without (pre-)preparation 46 d after host infection in Syrian hamsters (*Mesocricetus auratus*) and hepatoportal perfusion. *Schistosoma mansoni* samples were provided by C. Grevelding, Justus Liebig University Giessen.

3D optical microscope images of the sample surfaces were obtained with a Keyence VHX-5000 digital microscope (Keyence Deutschland GmbH, Neu-Isenburg, Germany) equipped with a VH-Z250R objective lens for comparison. No washing steps were applied before matrix application. A solution of 7 mg/ml  $\alpha$ -cyano-4-hydroxycinnamic acid (CHCA; 97% purity, Sigma-Aldrich, Steinheim, Germany) in acetone/water (0.2% TFA) 1:1 v/v was freshly prepared for matrix application. A volume of 70  $\mu\text{l}$  CHCA matrix solution was sprayed onto the sample surface using an ultrafine pneumatic sprayer system ("SMALDIPrep," TransMIT GmbH, Giessen, Germany). A second set of samples was prepared by pneumatically spraying 100  $\mu\text{l}$  of a freshly prepared 30 mg/ml 2,5-dihydroxybenzoic acid (DHB, 98% purity, Sigma-Aldrich, Steinheim, Germany) acetone/water (0.2% TFA) 1:1 v/v matrix solution onto the sample surface using the same device.

**MSI.** The mass spectrometer was operated in positive ion mode at a mass resolution of 140,000 at  $m/z$  200. The mass range used for the MSI experiments was between  $m/z$  50–1,200 depending on sample and analyte type. External calibration was performed before each measurement, and this resulted in a mass accuracy of better than 2 p.p.m. The scan speed for topographic surface scanning alone without MALDI analysis was 2.0 pixels/s; whereas for the pixel-wise autofocusing AP MALDI measurements, the speed decreased to 0.6 pixels per second (0.8 pixels/s for MSI without

autofocus). The laser energy of the MALDI MSI laser was set to 0.9–1.3  $\mu\text{J}$  per laser pulse, depending on matrix type, sample type and intended ablation spot size. Laser beam energy was measured in the sample plane with a laser power meter (FieldMaxII-TOP, Coherent, Dieburg, Germany). The nitrogen laser was operated at 60 Hz, and 30 laser pulses were applied per pixel.

**Data analysis.** Topographic data were stored in a matrix file. The data matrix entries contained the  $z$ -axis position of the sample stage—i.e., the topographic information—whereas the row and column counters encoded for the pixel number—i.e., the lateral information. In-house-developed MATLAB scripts (**Supplementary Software**) were used to reconstruct the topographic data and generate topography images. The lowest measured  $z$ -axis position was subtracted from the topographic data in order to report positive height differences. MS data analysis was performed using MIRION<sup>25</sup> imaging software and in-house-developed MATLAB scripts. The ion selection bin width ( $\Delta m/z$ ) of the images, generated from the MS data set for untargeted compound analysis, was set to  $\Delta m/z = 0.01$ . All MS images were generated without further image processing steps such as smoothing, interpolation or TIC normalization; and an image bin width of  $\pm 2$  p.p.m. was used. MS images were normalized to the base pixel (highest intensity) per image (i.e., per  $m/z$  bin). MIRION images were exported as \*.bmp files and subsequently imported,

processed and combined with the topographic data by MATLAB scripts for 3D surface MS image formation. Resulting images were adjusted in brightness and contrast for optimal visibility. Compounds were assigned based on accurate mass measurements with a mass tolerance of less than 2 p.p.m., and we employed METLIN based on database searches<sup>26</sup> and MS<sup>2</sup> experiments (isolation width  $\Delta m/z = 0.4$ ; collision energy settings NCE = 25).

**Code availability.** MIRION and MATLAB executable code is available as **Supplementary Software**.

**Data availability statement.** The data sets generated and/or analyzed during the current study are available from the corresponding author on reasonable request. Database search results are available as **Supplementary Data**. Source data for **Figures 1** and **2** are available. A **Life Sciences Reporting Summary** is available.

21. Guenther, S., Koestler, M., Schulz, O. & Spengler, B. *Int. J. Mass Spectrom.* **294**, 7–15 (2010).
22. Koestler, M. *et al. Rapid Commun. Mass Spectrom.* **22**, 3275–3285 (2008).
23. Kompauer, M., Heiles, S. & Spengler, B. *Nat. Methods* **14**, 90–96 (2017).
24. Kompauer, M., Heiles, S. & Spengler, B. *Protocol Exchange* <http://dx.doi.org/10.1038/protex.2017.103> (2017).
25. Paschke, C. *et al. J. Am. Soc. Mass Spectrom.* **24**, 1296–1306 (2013).
26. Smith, C.A. *et al. Ther. Drug Monit.* **27**, 747–751 (2005).